Journal of Chromatography A, 1566 (2018) 124–134

Contents lists available at ScienceDirect

Journal of Chromatography A

journal homepage: www.elsevier.com/locate/chroma

Ionic liquid-coated alumina-pretreated micro gas chromatography columns for high-efficient separations

Bishnu P. Regmi, Ryan Chan, Arsalan Atta, Masoud Agah*

VT MEMS Lab, Bradley Department of Electrical and Computer Engineering, Virginia Tech, Blacksburg, VA 24061, United States

ARTICLE INFO

Article history:
Received 24 April 2018
Received in revised form 22 June 2018
Accepted 24 June 2018
Available online 25 June 2018

Keywords:
Micro GC
Separation columns
Atomic layer deposition
Alumina
Ionic liquids
Plate number

ABSTRACT

These studies demonstrate the influence of an intermediate layer of aluminum oxide on the separation performance of a room temperature ionic liquid (RTIL)-coated gas chromatography silicon microcolumn. A 1 m long semipacked column having 190 μm wide and 240 μm deep rectangular cross-sectional channels with embedded arrays of micro pillars was microfabricated. A thin layer of alumina was then deposited on the surface of the channels via atomic layer deposition. Following the alumina deposition, the channels were coated with an RTIL. The separation performance of the RTIL-coated columns with and without the alumina layer was evaluated by measuring the separation efficiency and peak capacity. A substantial increase in separation efficiency was observed in the presence of the alumina layer. The alumina-pretreated columns, at optimum flow rate, exhibited as high as 8000 plates per meter, which is a 2.1-fold increase as compared to the column with no alumina layer. It is inferred that alumina coating promotes the formation of a more uniform RTIL film, thereby enhancing the separation efficiency. The peak production rates of alumina-RTIL columns for temperature-programmed separation were found to be 0.80–1.1 peaks per second, which is an improvement compared to silicon-RTIL columns. The separation performance of these columns were further evaluated by separating a standard 21-component mixture of hazardous organic compounds, a sample of kerosene, diesel, and B20 biodiesel. These studies open up new possibilities of enhancing the separation efficiency of microcolumns by coating silicon surface with a suitable material prior to depositing an ionic liquid.

1. Introduction

Increasing demands for on-site analysis of chemicals, including pollutants, drugs, explosives, chemical warfare agents, petroleum products, and plant emissions, have driven the development of many portable or handheld analytical instruments. Among these portable devices, a micro gas chromatography system is one of the fastest growing technologies for trace-level analysis of complex chemical mixtures. The conventional gas chromatograph (GC) is bulky, fragile, energy intensive (power requirement of 2000–3000 volt-amperes) [1], and often requires long analysis time. Hence, these instruments are appropriate in conventional centralized laboratory settings. With an aim to reduce the size of the conventional GC, Terry et al. [2] introduced the concept of miniaturized GC in 1979. The authors fabricated major components in silicon by employing photolithography and chemical etching to dramatically reduce the size the GC system. Considerable research has been conducted to develop individual microfarbicated components and integrate these components by different investigators specifically in the past 25 years [3–44]. Currently, a number of commercial companies are producing portable GC systems, which include FROG-5000 of Defiant Technologies, Inc. [45], Micro GC Fusion of INFICON, Inc. [46], portable zNose of Electronic Sensor Technology Inc. [47], ChromPix of APIX Analytics, SA [48], and NovaTest P100 of Nanova Environmental, Inc. [49].

A separation column is a vital component that plays a central role in successful analytical separations. Two types of columns—capillary columns of circular cross sections [6,48,49] and chip-based columns of rectangular cross sections [2–5]—have been pursued by both research and commercial labs. Polyimide-clad fused silica capillary tubing has been widely employed, because it provides higher resolution due to the formation of a more uniform film of the stationary phase. Chip-based silicon columns, known as microcolumns, are an excellent alternative to these conventional capillary columns. Microcolumns are prepared by fabricating microchannels into silicon chips followed by anodic bonding of silicon with glass. The microchannels in silicon are often rectangular in cross section because of certain limitations associated with the fabrication processes. Chip-based separation columns offer a number of unique advantages: (i) they offer reduced heating and cooling times due to better thermal properties, (ii) they have significantly reduced size, and they can be heated using relatively low power, (iii)

* Corresponding author. Tel.: +540 231 2653; fax: +540 231 3362.
E-mail address: agah@vt.edu (M. Agah).

https://doi.org/10.1016/j.chroma.2018.06.058
0021-9673/

they can be batch produced thereby lowering the manufacturing cost; (iv) dead volumes and cold spots can be minimized by monolithic integration of microcolumn with other components; and (v) provide an opportunity to fabricate regularly arranged structures inside the channels to enhance separation performance [7–12]. In addition, it has been theoretically predicted that high-aspect-ratio rectangular columns potentially offer high resolution and can deliver higher flows [50].

The separation efficiency of microcolumn is low due to short and non-cylindrical channels [13]. Considerable efforts have therefore been made to increase separation efficiency, sample capacity, and peak capacity by exploring new column designs or coating techniques [11–24]. In an effort to increase the separation efficiency and sample capacity, our group introduced the concept of semipacked columns (SPCs), which comprise an array of micropillars embedded within the rectangular channels [12]. Along the same line, Jespers et al. [14] recently developed a chip-based multicapillary column with interconnected channels to increase the separation efficiency and sample capacity. A wide range of materials, including polymers [14–16], carbon nanotubes [17], sputtered silica and graphite [18], silica nanoparticles [19], alumina [20,21], and self-assembled monolayers on gold [22], have been investigated as stationary phases in GC columns fabricated by microelectromechanical systems (MEMS) technology. Despite these developments, the search for more flexible stationary phase materials for microcolumns is an ongoing interest. One of the versatile classes of stationary phase materials are room temperature ionic liquids (RTILs)—organic salts that remain in the liquid state at room temperature. RTILs possess high viscosity, high thermal stability, and low vapor pressure making them attractive stationary phases in gas chromatography. RTILs show multitude of solvation interactions which can be easily tuned, and hence these materials can be easily tailored to the separation of desired mixtures [51]. An interesting feature of RTILs is that they can separate both polar and non-polar analytes [52,53].RTIL-coated conventional capillary columns are currently being commercialized, and these columns have been increasingly used in the separation of a wide range of chemical mixtures, including enantiomeric mixtures, flavor and fragrance compounds, petrochemicals, and fatty acid methyl esters [51,54–58]. A comprehensive summary on the use of RTILs in wall-coated open-tubular columns has been provided by Poole and Lenca [59]. More recently, Collin et al. [28] deposited an RTIL in a microcolumn and demonstrated the feasibility of the column as a second-dimension column in 2D micro GCs. We coated the channels of semipacked columns (SPC) with two commercial RTILs and used these columns for the separation of a range of polar and non-polar compounds [60]. These columns exhibited symmetrical peaks (tailing factor: 0.92–1.76) with reasonable separation efficiencies (2100–2300 plates per meter).

In the present study, we explored the influence of surface modification of the SPC channels prior to coating with an RTIL. The particular focus of these studies has been to enhance the separation efficiency using batch-fabricated columns provided by MEMS technology. The surface of the silicon channels, including the pillars, were modified by depositing a 10 nm thick layer of aluminum oxide via atomic layer deposition. A thin layer of an RTIL was subsequently deposited on the surface of the oxide film by using dynamic coating method; and the separation performance of these columns was evaluated by measuring the separation efficiency as a function of flow rate of the mobile phase. Peak capacities of these columns for temperature-programmed separation have been evaluated. These columns were further characterized by separating a number of complex chemical mixtures, including a 21-component mixture of hazardous organic compounds, a sample of kerosene, diesel, and 20% soy biodiesel.

2. Experimental section

2.1. Materials

Two RTILs, namely, 1-butylpyridinum bis(trifluoromethylsulfonyl)imide ([BPyr][NTf_2]) and trihexyltetradecylphosphonium bis(trifluoromethylsulfonyl)imide ([P_{66614}][NTf_2]) were obtained from Ionic Liquids Technologies, Inc. (Tuscaloosa, AL, US). Silicon wafers (n-type, 4 in diameter, 500 μm thickness, single side polished) and Borofloat wafers (4 in diameter, 500 μm thickness) were purchased from University Wafer, Inc. (Boston, MA, US). Fused silica capillary tubes with 100 μm internal diameter and 200 μm outer diameter were obtained from Polymicro Technologies, LLC. (Lisle, IL, US). A J-B Weld two-part epoxy system was obtained from a local store. Acetone was obtained from Spectrum Chemical Mfg. Corp. (New Brunswick, NJ, US) Benzene, n-hexane, n-heptane, n-octane, n-nonane, toluene, ethylbenzene, p-xylene, m-xylene, o-xylene, isobutylbenzene, n-butylbenzene, styrene, benzyl chloride, 2-chlorotoluene, 2,5-dichlorotuluene, 1,2-dichlorobenzene, 1,2,4-trichlorobenzene, naphthalene, 2-nitrotoluene, 3-nitrotoluene, 4-nitrotoluene, and a standard mixture of C7–C30 saturated alkanes (in hexane) were obtained from Sigma Aldrich (St Louis, MO, US). Fatty acid methyl esters (FAME#1) and biodiesel blend were obtained from Restek Corporation (Bellefonte, PA, US). Samples of Crown 1-K Kerosene and diesel were obtained from local stores. Air, methane, and ultrapure helium were purchased from Airgas, Inc. (Christiansburg, VA, US). Ultrapure hydrogen for flame ionization detector (FID) was produced by using Parker Domnick Hunter (Gateshead, UK) hydrogen generator. All of the above chemicals were used without any further purification.

2.2. Column fabrication and coating

The detail protocol for the fabrication of the columns is given in the Supplementary Data. Geometrical features of the fabricated columns were analyzed using LEO (Zeiss) 1550 Scanning Electron Microscope (SEM). Following wafer dicing and attaching the capillary tubes to the columns, we coated them with selected stationary phases. We used two RTILs, i.e., [BPyr][NTf_2] and [P_{66614}][NTf_2] because they exhibit high thermal stability, are commercially available, and possess different polarity. The RTILs were deposited inside the channels of the separation columns using a dynamic coating procedure at room temperature by employing a freshly prepared solution of an RTIL in acetone. The concentration of RTIL used was 0.8% (w/v). The entire column was first filled with the solution of RTIL, and the solution was removed by using nitrogen gas at a pressure of 10 psi. After removing the bulk of the solution, the column was placed under vacuum to evaporate the residual solvent in quiescent conditions. After coating, approximately half a foot of capillary tubing was removed from each side to make 15 cm of fused capillary capillaries on each side of the chip. The internal diameter of the capillaries was 100 μm, and these were connected to the chip using J-B Weld two-part epoxy system.

2.3. Data acquisition

The separation experiments were performed on an Agilent 7890A GC (Agilent Technologies, Inc. Santa Clara, CA, US) system equipped with an automatic sampler (7693A), two split/splitless inlets, and two flame ionization detectors (FIDs). Helium gas was used as a mobile phase. Before running the separation experiments, each column was conditioned by heating, under the inlet pressure of 10 psi, from 30 to 200 °C at a ramp rate of 2 °C per min and holding at 200 °C for additional 15 min. The temperature of the inlet was held at 280 °C and the detector at 300 °C during column con-

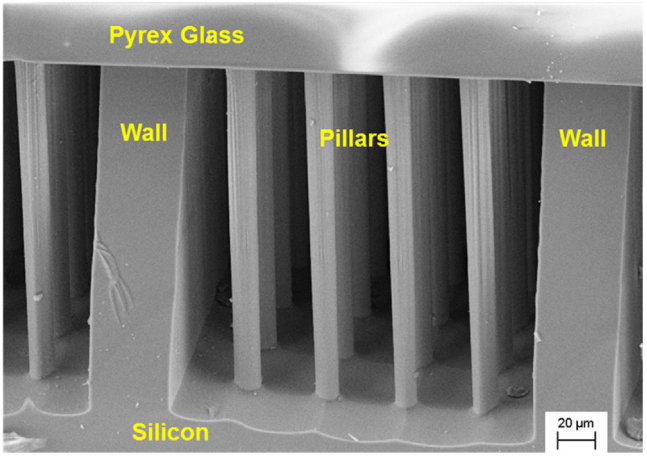

Fig. 1. SEM image of a section of semipacked column.

ditioning and subsequent chromatographic separations. The data acquisition rate of the FID was 50 Hz. The data were collected and analyzed using the Agilent ChemStation Edition C.01.04.

3. Results and discussions

3.1. Characterization of the separation columns

The microcolumn designed was 1 m long, 240 μm deep, 190 μm wide comprising 20 μm cylindrical pillars with an interpillar distance of 42 μm. The layout of the channels was serpentine. Fig. 1 shows the SEM image of a section of microcolumn used in these studies. The SEM image shows that the pillars are essentially non-tapered; however, the diameter is approximately 15 μm, resulting in an increase in interpillar distance. The RTIL films were not clearly observed, and we were unable to estimate the film thickness.

3.2. Evaluation of column separation efficiency

The column efficiency was evaluated by measuring the number of theoretical plates (N) and height equivalent to a theoretical plates (HETP) under different linear velocities of mobile phase. The hold-up time was measured by using methane as an unretained marker. The values of N and HETP were determined using naphthalene as a probe at a constant temperature of 100 °C. We selected naphthalene as a probe because majority of the previous studies have used this compound to evaluate the column efficiency of RTIL-coated columns [59]. The different parameters were calculated from the experimental chromatograms using the following equations:

$$\bar{u} = \frac{L}{t_M} \quad (1)$$

$$k = \frac{t_R - t_M}{t_M} \quad (2)$$

$$N = 5.545 \left(\frac{t_R}{w_h}\right)^2 \quad (3)$$

$$HETP = \frac{L}{N} \quad (4)$$

where, $\bar{u}$ is average carrier-gas linear velocity, L is the length of a column, t_M is hold-up time, t_R is the retention time of naphthalene, N is the number of theoretical plates (or plate numbers), w_h is the peak width at half height of the naphthalene peak.

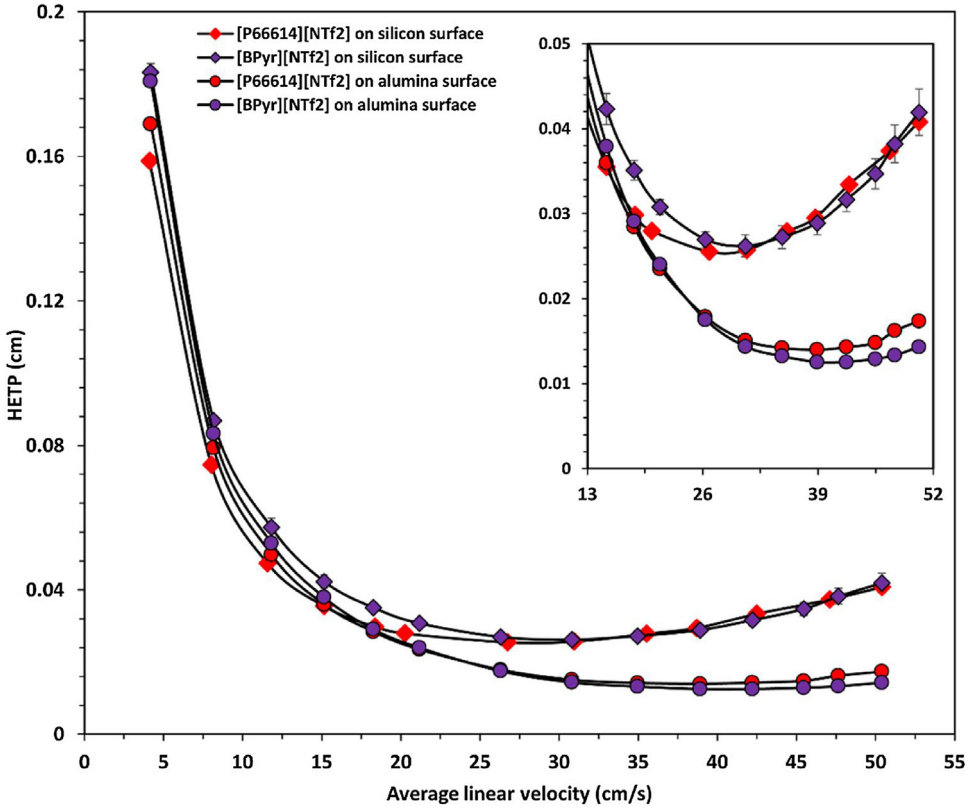

Fig. 2. Variation HETP as a function of average linear velocity of mobile phase (helium) for different columns prepared by immobilizing RTILs on silicon and alumina surfaces. Legend shows the type of interface. The error bars indicate the standard deviations for three different independently coated columns using 0.8% (w/v) solution of [BPyr][NTf_2] (shown for silicon surface only). Inset shows magnified view of a region. The HETP values were determined using naphthalene as a probe under isothermal conditions. Chromatographic conditions for each column: injection volume 0.1 μL (0.5% w/v of naphthalene in hexane), split ratio 200:1, inlet temperature 280 °C, detector temperature 300 °C, and oven temperature 100 °C. The average velocity was calculated my using methane as an unretained solute.

Table 1
Comparison of the Retention Time (t_R), Resolution (R_s), and Tailing Factor (T_f) for Columns Coated with [BPyr][NTf_2] on Silicon and Alumina Surfaces.

Peak Number	Compounds	[BPyr][NTf_2] coated on silicon surface			[BPyr][NTf_2] coated on alumina surface		
		t_R(min)	R_s	T_f	t_R(min)	R_s	T_f
1	Heptane	0.068		na	0.070		na
2	Octane	0.076	1.24	na	0.079	1.38	na
3	Nonane	0.093	1.89	1.29	0.097	2.28	1.13
4	Benzene	0.143	4.36	1.34	0.145	5.35	1.29
5	Toluene	0.261	6.54	1.30	0.262	9.66	1.16
6	Ethylbenzene	0.434	5.74	1.22	0.435	8.80	1.02
7	p-Xylene	0.530	na	na	0.516	na	na
8	m-Xylene	0.530	na	na	0.532	na	na
9	o-Xylene	0.681	na	1.18	0.680	na	1.08
10	2-Chlorotoluene	0.764	2.17	na	0.768	3.63	na
11	Isobutylbenzene	0.808	1.09	na	0.812	1.75	na
12	Styrene	0.851	1.09	na	0.851	1.66	na
13	Butylbenzene	1.028	4.80	1.05	1.027	7.70	0.82
14	1,2-Dichlorobenzene	1.163	3.62	1.03	1.165	5.88	0.91
15	2,5-Dichlorotoluene	1.290	3.35	1.02	1.289	5.25	0.88
16	1,2,4-Trichlorobenzene	1.445	4.02	0.92	1.446	6.31	0.78
17	Benzyl chloride	1.545	2.68	1.28	1.533	3.56	1.26
18	Naphthalene	2.338	21.1	1.07	2.318	32.2	1.00
19	2-Nitrotoluene	2.426	2.24	1.00	2.420	3.93	1.02
20	3-Nitrotoluene	2.528	2.59	0.96	2.529	4.08	1.01
21	4-Nitrotoluene	2.640	2.84	1.00	2.644	4.32	1.22

While static coating is typically preferred, we used the dynamic coating method because our preliminary experiments on static coating showed bubble formation during vacuum evaporation. We first investigated the repeatability in the production of the separation columns by independently coating three silicon columns using 0.8% (w/v) of [BPyr][NTf_2], and the number of theoretical plates were determined using naphthalene at 100 °C under different average linear velocity of the mobile phase. Fig. 2 shows the variation of HETP as a function of average linear velocity of the carrier gas, i.e. Golay Plots, where the error bars indicate the standard deviation in HETP of three independent measurements. The relative standard deviations were found to be between 1.3 to 6.7% indicating very high repeatability in the preparation of separation columns. The optimum velocity (u_{opt}) of the carrier (helium) gas was found to be 31 cm.s^{-1} (k for naphthalene 8.9 at inlet pressure 25 psig), with the maximum number of theoretical plates (N_{max}) of 3822 ± 195 per meter. We then modified the silicon surface of the columns with aluminum oxide via atomic layer deposition. The RTIL was immobilized on these modified surfaces, and the Golay plot was generated (Fig. 2). Here, N_{max} was found to be 8000 per meter at u_{opt} of 39 cm.s^{-1} (k for naphthalene 8.2 at inlet pressure of 35 psig) indicating changes in both N_{max} and u_{opt}. The columns were also coated with another RTIL, [P_{66614}][NTf_2], and Golay plots were generated (Fig. 2). The silicon-[P_{66614}][NTf_2] column showed N_{max} of 3917 plates per meter at u_{opt} of 27 cm.s^{-1} (k for naphthalene 7.2 at inlet pressure of 25 psig) and the alumina-[P_{66614}][NTf_2] column exhibited N_{max} of 7158 plates per meter and u_{opt} of 39 cm.s^{-1} (k for naphthalene 10.5 at inlet pressure of 35 psig). These observations indicate that highly efficient separation columns can be designed by suitably modifying the silicon surface prior to RTIL deposition. It is obvious from Fig. 2 that the Golay curves for silicon-RTILs show steeper slopes compared to the curves for alumina-RTILs at higher flow rates. In this region, the mass transfer (C term the van Deemter equation) dominates, and this term varies with the square of the film thickness. These observations indicate that thinner RTIL films are formed on alumina surfaces as compared with silicon surfaces. The higher value of u_{opt} for alumina-RTIL columns is also a consequence of thinner films. We also dynamically coated a capillary fused silica capillary of internal dimeter of 100 μm using 0.8% of [BPyr][NTf_2]. The separation efficiency was determined at 50 and 100 °C using naphthalene as a probe. The number of theoretical plates at optimum flow rate was found to be 850 plates per meter. While N_{max} for this capillary column is similar to that reported by Collin et al. [28], an improvement is expected on pretreating the capillary tubing prior to coating with an RTIL [59]. However, this is not the focus of these studies.

It is important to mention here that for high-aspect-ratio columns, the separation efficiency depends on the narrower dimension of the column; smaller the dimension greater is the efficiency [50]. Another factor that influences the separation efficiency and is relevant to the present studies is the film thickness; thinner the film greater is the efficiency. A careful analysis of the literature reveals that it is more challenging to obtain more uniform film of a polar stationary phase [28,61]. For example, in the studies recently reported by Collin et al. [28], a microcolumn having a cross-sectional area of 250 μm × 140 μm on static coating with OV-1 (a nonpolar stationary phase) exhibited 3800 plates per meter; in contrast, a microcolumn of 46 μm × 150 μm in cross section on coating with an RTIL (a polar stationary phase) exhibited only 1300 plates per meter [28]. The studies by Collin et al. involved pretreatment of column with sodium chloride prior to coating with the RTIL. During our preliminary experiments, we could not improve the separation efficiency on pretreating the columns with sodium chloride; hence, we chose to coat with alumina. Considering the polar nature of RTILs, the number of theoretical plates obtained in the present studies represents a substantial improvement. As compared to our previous studies [60], we observed some improvement in separation efficiency for the untreated silicon columns likely due to the formation of more vertical pillars. By coating the surface of silicon with alumina prior to depositing a film of RTIL, the separation efficiency is shown to increase by approximately 1.8–2.1 fold. The separation efficiency offered by alumina-RTIL is approximately 90 percent higher than that offered by alumina layer functionalized with silane [20]. The retention times of 21 different compounds for [BPyr][NTf_2] coated on silicon surface and alumina surface are shown in Table 1. The retention times for these compounds are very similar for these two columns indicating similar amount of coating materials was deposited. An attempt to characterize the films using scanning electron microscopy was not successful. Since the amount of coating material is similar, better surface coverage will lead to thinner films leading to better separation efficiency.

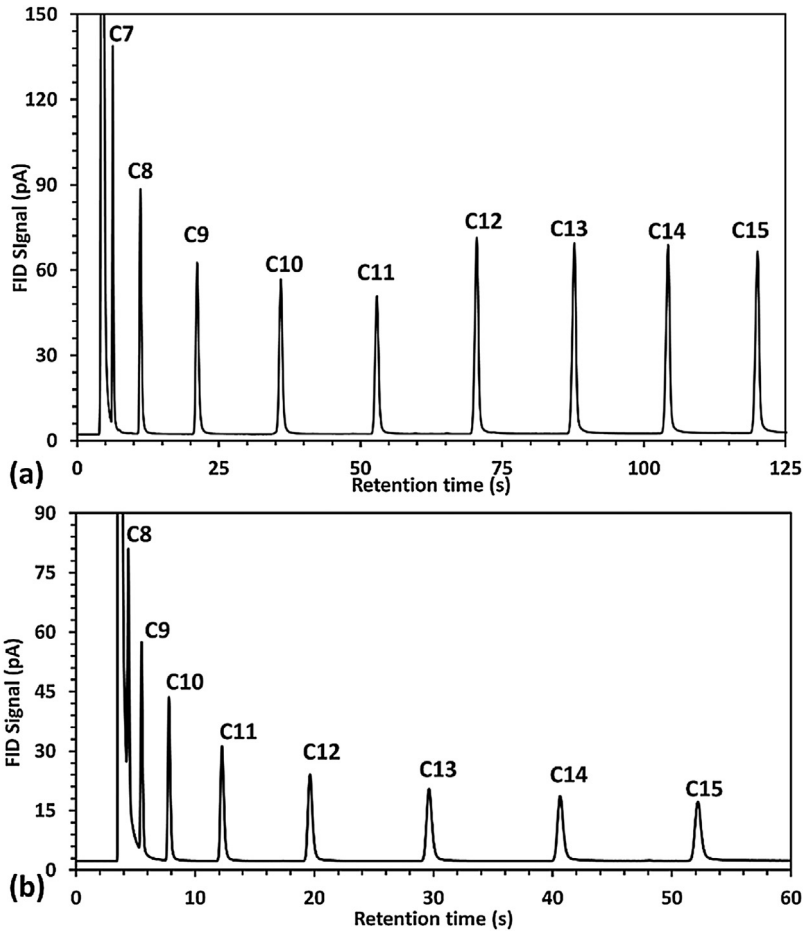

Fig. 3. Temperature-programmed separation of normal alkanes using alumina-RTIL columns: (a) n-C7–n-C15 (in hexane) using alumina-[P_{66614}][NTf_2], initial temperature 30 °C; ramp rate 50 °C per minute, flow rate 39 cm per second; (b) n-C8–n-C15 using alumina-[BPyr][NTf_2], other conditions same as in a.

3.3. Evaluation of peak capacity

A basic metric to compare the performance of temperature-programmed separation is peak capacity (n_p). The peak capacity for the retention range $n{-}C_x$ to $n{-}C_y$ is calculated by using the following equations [62]:

$$n_p = \sum_{n=x}^{n=y} (TZ + 1) \tag{5}$$

$$TZ = \frac{t_{R(n+1)} - t_{R(n)}}{w_{h(n)} + w_{h(n+1)}} - 1 \tag{6}$$

where TZ is Trenzahl number; $t_{R(n)}$ and $t_{R(n+1)}$ are the retention times of two adjacent normal alkanes; and $w_{h(n)}$ and $w_{h(n+1)}$ are full width at half height of the corresponding peaks. The temperature-programmed chromatograms for the separation of normal alkanes using alumina-RTIL columns are shown in Fig. 3a–b. There was baseline separation for all compounds (the first pair showed baseline separation if there was no overloading of the first peak). The alumina-[P66614][NTf2] column was able to separate n-C7–n-C15 in 122 s (Fig. 3a) at the optimum flow and ramp rate of 50 °C per minute. The peak capacity was found to be 98 with a peak production rate of 0.80 peaks per second. Similarly, the alumina-[BPyr][NTf2] column was able to separate n-C8–n-C15 in 53 s (Fig. 3b) with a peak capacity of 58 and with a peak production rate of 1.1 peaks per second. Under similar conditions, the peak production rate with alumina non-pretreated columns was found to be 0.51 peaks per second (Figs. S2 and S3, Supplementary Data), indicating 1.6–2.2-fold improvement in peak production rate due to alumina pretreatment prior to the deposition of RTILs. Previously reported values of peak capacities for PDMS-coated microfabricated columns were 167 peaks in 216 s (0.77 peaks per second) [14] and 100 peaks in 500 s (0.2 peaks per second) [62].

3.4. Separation of complex mixtures

Following the evaluation of the separation efficiency and the peak capacity, the different columns were utilized for the separation of complex mixtures. The first test mixture separated comprised a 21-component standard mixture composed of saturated alkanes, aromatic hydrocarbons, aromatic halides, and nitroaromatic compounds. The boiling point of the compounds range from 80 °C (heptane) to 238 °C (4-nitrotoluene). These hazardous chemical compounds are widely distributed in different environmental compartments, including air, water, and soil. A mixture of these compounds were prepared by mixing similar amounts, and 0.1 μL of the neat mixture was injected with a split ratio of 400:1. The peaks in the chromatograms were identified by injecting a 5% solution of the component in hexane. Fig. 4a–b shows chromatograms for the separation of the 21-component mixture using the columns coated with [BPyr][NTf_2] on alumina and silicon surfaces. The retention time, tailing factor (at 5% peak height), and the resolution between different peaks are shown in Table 1. The resolution values given the table refer to the resolution between the peak of interest and the preceding peak. The alumina non-pretreated column gave the resolution values of 1.09 to 21.1, while the alumina pretreated column exhibited the resolution values of

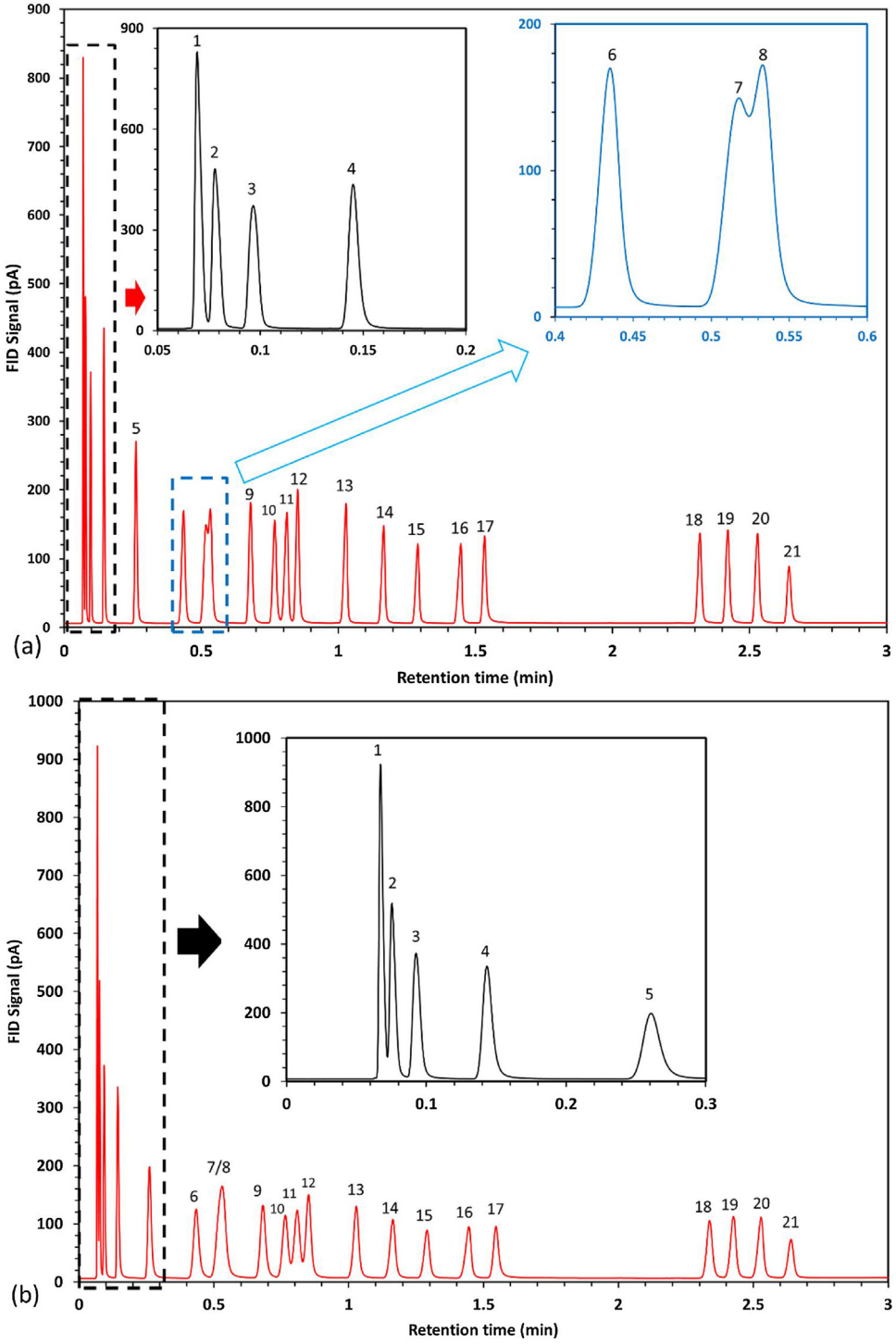

Fig. 4. Chromatograms showing the separation of a 21-component mixture of organic compounds using a column prepared by depositing [BPyr][NTf_2] on (a) alumina surface and (b) silicon surface. Chromatographic conditions: injection volume 0.1 μL, split ratio 400: 1, inlet pressure 25 psi for 0.5 min and then ramped to 35 psi at the rate of 60 psi/min, oven temperature 30 °C for 0.5 min and then ramped at the rate of 40 °C/min–130 °C. The insets show magnified view of the selected regions. The peak numbers correspond to the compounds shown in Table 1.

1.38 to 32.2. The peaks were found to be symmetrical for both the columns, with tailing factors ranging from 0.78 to 1.34, and the alumina pretreatment did not compromise the peak symmetry. The tailing displayed in our micro GC columns is slightly inferior to that observed in fused silica capillary columns coated with ILs [63]. The primary cause of peak tailing in microcolumns is surface adsorption, which is due to the presence of active sites (such as hydroxyl groups on silica, silicon, and alumina) on the walls of the columns [61,64]. Other causes of peak tailing are unswept (dead) volumes, improper column installation, improperly cut capillary, and non-linear retention [64]. Our RTIL-coated SPCs show significant improvement in peak symmetry when compared to previous studies in which considerable tailing even for n-alkanes has been reported [15,18,65]. It should be noted that peak tailing significantly compromise the resolution [66]. An improvement in resolution was observed due to alumina pretreatment; we were

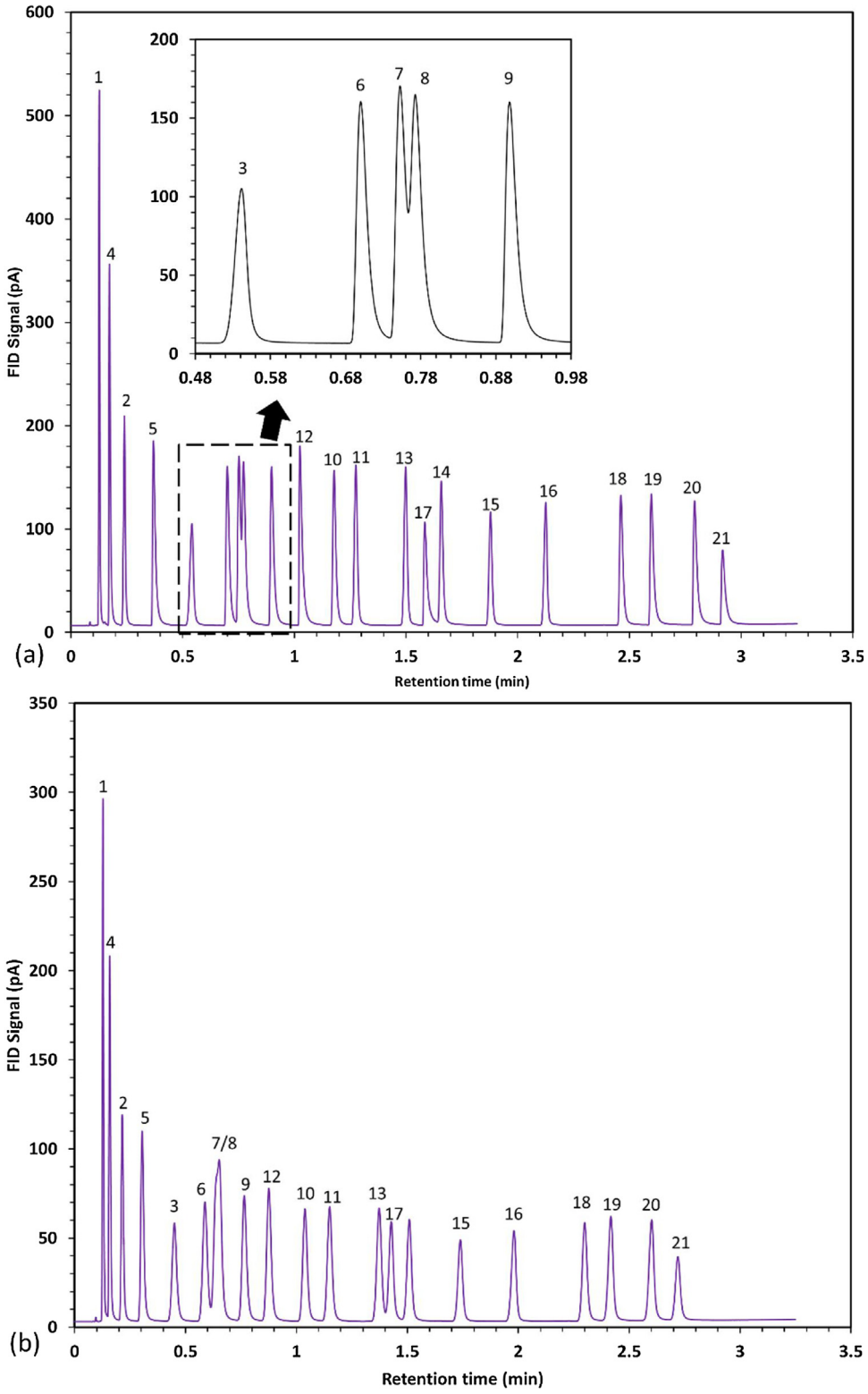

Fig. 5. Chromatograms showing the separation of a 21-component mixture of organic compounds using a column prepared by depositing $[P_{66614}][NTf_2]$ on (a) alumina surface and (b) silicon surface. Chromatographic conditions: same as those of Fig. 4 except that the column was heated up to 140 °C. The peak numbers correspond to the compounds shown in Table 1. Note the order of elution is altered as compared to that of Fig. 4.

able to partially separate p- and m-xylenes, which was not possible with columns containing the silicon surface. The nature of the surface (silicon or alumina) did not change the order of the elution for these 21 compounds, and the retention times were found to be very similar. We also attempted to separate these 21 compounds using uncoated columns or columns coated with a very thin film (approximately 8-fold lower) of this RTIL. We saw retention but not a good separation (Figs. S4–S7, Supplementary Data), indicating that an RTIL is required for useful separations. We replaced the RTIL $[BPyr][NTf_2]$ with another RTIL, i.e., $[P_{66614}][NTf_2]$ and used

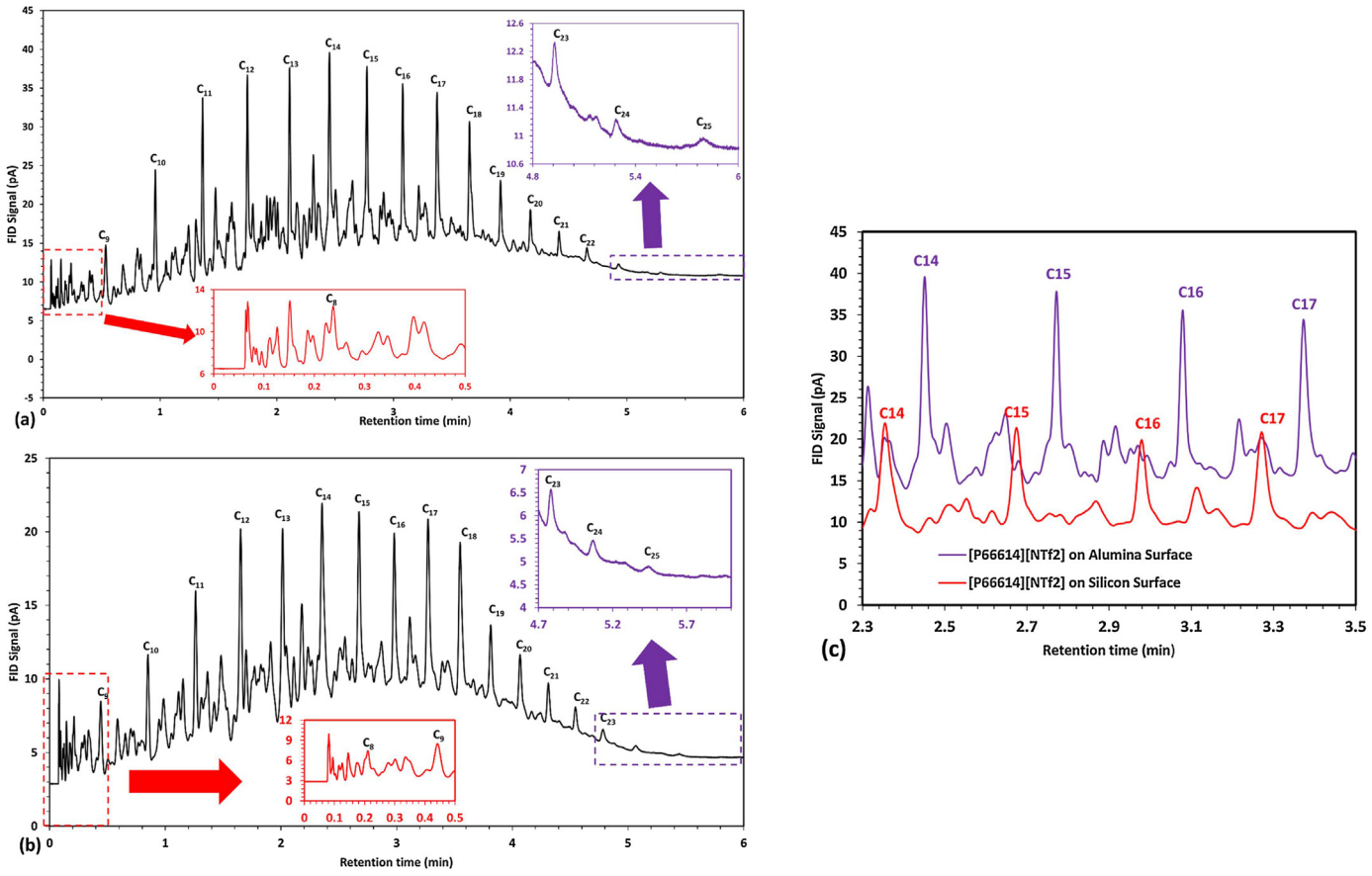

Fig. 6. Chromatograms showing the separation of a diesel sample (a) using a column coated with $[P_{66614}][NTf_2]$ on alumina surface, (b) using a column coated with the same RTIL on silicon surface, and (c) an overlay of the chromatograms from a and b in a selected region. Chromatographic conditions: injection volume 0.1 μL, split ratio 400: 1, inlet pressure 25 psi for 0.5 min and then ramped to 35 psi at the rate of 60 psi/min, oven temperature 30 °C for 0.5 min and then ramped at the rate of 40 °C/min to 190 °C and held at 190 °C for 1.5 min. The insets show the magnified views of the selected regions. The major peaks were identified by comparing the retention time of the peaks to a standard mixture of (C_7–C_{30}) n-alkanes.

the column to separate these 21 compounds. The elution order of some of the compounds have been found to be changed (Fig. 5a–b) on changing the RTIL; however, the elution order did not change on altering the surface, indicating that the selectivity is dependent essentially on the RTIL and the surface effects could be very low in determining the selectivity. The retention time, tailing factor, and the resolution between different peaks have been summarized in Table S2 (Supplementary Data). Some differences in retention time could be seen possibly due to slightly different amount of RTIL deposited inside the column. The silicon-$[P_{66614}][NTf_2]$ column exhibited symmetrical peaks, while some peaks including styrene, benzyl chloride and nitrotoluenes were unsymmetrical with tailing factor 2.6 to 3.2 in alumina pretreated column. These observations support that the surface activity is the primary cause of peak tailing. Again, alumina pretreated column exhibited increased resolution between the peaks. The changes in the retention order on altering the RTILs can be understood by considering the solute descriptors and the strengths of interactions of the stationary phase [67,68]. ILs show abilities to undergo multiple solvent interactions with the solute molecules. These interactions include interaction through nonbonding and π-electrons, dipole-type interactions, hydrogen bond (basicity and acidity), and cohesion and dispersion interaction. The interaction parameters of an RTIL depends on its cation-anion combination, and the types and relative strengths of interactions between an RTIL and analyte determines the retention time.

Finally, our columns were tested for the separation of biodiesel and petroleum products. GC has been widely used as a key analytical tool for the analysis of biodiesel and petroleum products [51,58,69–72]. GC has been also used in the analysis of biodiesel and petroleum-based accelerants in case where arson is suspected [73–75]. Development of portable devices to analyze biodiesel and petrochemicals will offer possibilities of rapid and on-site analysis of these products. It has been shown that ionic liquid-coated capillary columns are useful in the determination of hydrocarbon group types of diesel fuels [58], separation of aliphatic hydrocarbons from kerosene [51], and separation of fatty acid methyl esters in biodiesel [72]. Due to the presence of long chain alkyl groups, the ionic liquid $[P_{66614}][NTf_2]$ is able to exhibit nonspecific dispersive interactions, and hence shows potential to separate aliphatic hydrocarbons [51]. Therefore, the alumina-$[P_{66614}][NTf_2]$ column was used for the separation of hydrocarbons of diesel and kerosene. The major peaks in these products were located by comparing the retention time with a standard mixture of n-alkanes (Sigma-Aldrich, 49451-U Supelco, C7–C30 Saturated Alkanes). Fig. 6a–b shows the chromatograms for the separation of a sample of diesel using the columns coated with the RTIL on alumina and silicon surfaces, and Fig. 6c is an overlay of the two chromatograms from a selected region. Fig. 6c shows that the alumina-pretreated column produces sharper peaks and there is an increase in the number of peaks compared to the alumina non-pretreated column. Similar observations were seen for the separation of a sample of kerosene (Figs. S8–S10, Supplementary Data). The IL $[BPyr][NTf_2]$, which is more polar than the other IL, was used to separate FAMEs in 20% (1 part biodiesel in 4 parts diesel, i.e., B20) soy biodiesel. The major FAMEs reported in soy biodiesel are methyl palmitate (C16:00), methyl stearate

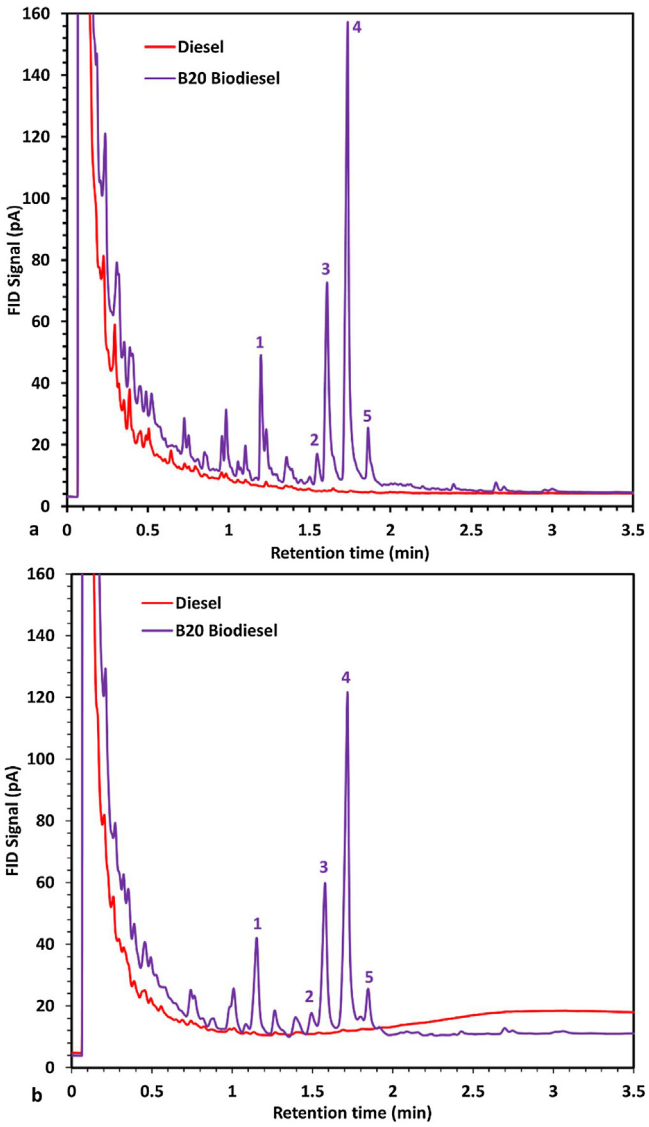

Fig. 7. Overlay of the chromatograms of the separation of diesel and B20 soy biodiesel using (a) the alumina-[BPyr][NTf_2] and (b) silicon-[BPyr][NTf_2] columns. The legend shows the identity of the test sample. Diosel:Biodisel (80:20) blend at a concentration of 5 mg per ml in dichloromethane was obtained from Restek Corporation. A 5 mg per ml solution of diesel in dichloromethane was prepared in the lab. Chromatographic conditions: injection volume 1 μL, split ratio 20: 1, inlet pressure 35 psig, oven temperature ramped from 100 °C at the rate of 40 °C/min to 200 °C and held for 1 min. The fatty acid methyl esters peaks were identified by comparing the retention time of the peaks to a standard mixture of fatty acid methyl esters (FAME #1 from Restek Corporation). The peak numbers correspond to: (1) methyl palmitate (C16:00), (2) methyl stearate (C18:00), (3) methyl oleate (18:01), (4) methyl linoleate (C18:02), and (5) methyl linolenate (18:03). For alumina-pretreated column, the resolution value between peaks 2 and 3 is 1.48, 3 and 4 is 3.34, and 4 and 5 is 3.77, while for non-pretreated column the values are 1.28, 2.73, and 2.86.

(C18:00), methyl oleate (18:01), methyl linoleate (C18:02), and methyl linolenate (18:03) [76]. Fig. 7a–b shows an overlay of chromatograms of B20 biodiesel and diesel, and it is evident that all of these FAMES are separated in less than 2 min with little interference from other hydrocarbons present in the biodiesel. An increased resolution can be seen with alumina-pretreated column as compared to the non-pretreated column.

4. Conclusions

These studies investigated the merits of using an intermediate layer of alumina on the separation performance of RTIL-coated silicon microcolumns. The alumina film was created via atomic layer deposition, and then an RTIL was coated on the alumina surface. The results of these studies demonstrate that such an intermediate layer enhances the separation performance of RTIL-coated semipacked columns. The separation efficiency, as measured by the number of theoretical plates, was found to be as high as 8000 plates per meter under optimal flow rate. For temperature-programmed separations, peak production rate was found to be between 0.80–1.1 peaks per second for alumina-pretreated column and 0.51 peaks per second for non-pretreated columns. A rapid separation of different complex mixtures were achieved. The alumina pretreatment indicated the formation of more homogeneous films of an RTIL resulting in an increase in separation efficiency. These results highlight the importance of silicon channel coating prior to the deposition of stationary for increasing the separation performance. These findings will be very beneficial for the development of miniaturized gas chromatography columns and hence portable gas chromatography systems. Due to the presence of alumina, these columns are not suitable for separation of active compounds like alcohols and ketones. The continuing work is directed at replacing the alumina layer by inert materials as well as deactivating the channel surfaces for the separation of more polar compounds.

Conflict of interest

The authors declare no conflict of interest.

Acknowledgements

The fabrication of separation columns were done at the Micro & Nano Fabrication Laboratory at Virginia Tech. The work was supported by the Bradley Department of Electrical and Computer Engineering and the National Science Foundation under the award ECCS-1711699.

Appendix A

The chip fabrication protocol; critical dimensions of the column channels; the Bosch process etch parameters; temperature-programmed separation of normal alkanes using silicon-RTIL columns; separations using uncoated columns or columns coated with a very thin film of RTILs; separation of a kerosene sample; and comparison of retention times, retention factors, and tailing factors for 21-component mixture using [P_{66614}][NTf_2]-coated columns are given in the supplementary data.

Appendix B. Supplementary data

Supplementary material related to this article can be found, in the online version, at doi:https://doi.org/10.1016/j.chroma.2018.06.058.

References

[1] J.V. Hinshaw, Preparing the laboratory for a gas chromatograph, in: Advanstar Communications 131 W FIRST ST, DULUTH, MN 55802 USA, 2003.
[2] S.C. Terry, J.H. Jerman, J.B. Angell, A gas chromatographic air analyzer fabricated on a silicon wafer, IEEE Trans. Electron. Devices 26 (1979) 1880–1886.
[3] A. Garga, M. Akbar, E. Vejerano, S. Narayanan, L. Nazhandali, L.C. Marr, M. Agah, G.C. Zebra, A mini gas chromatography system for trace-level determination of hazardous air pollutants, Sens. Actuators B 212 (2015) 145–154.
[4] G.C. Frye-Mason, R.J. Kottenstette, E.J. Heller, C.M. Matzke, S.A. Casalnuovo, P.R. Lewis, R.P. Manginell, W.K. Schubert, V.M. Hietala, R.J. Shul, Integrated chemical analysis systems for gas phase CW agent detection Micro Total Analysis Systems', vol. 98, Springer, 1998, pp. 477–481.
[5] C.J. Lu, W.H. Steinecker, W.C. Tian, M.C. Oborny, J.M. Nichols, M. Agah, J.A. Potkay, H.K.L. Chan, J. Driscoll, R.D. Sacks, K.D. Wise, S.W. Pang, E.T. Zellers,

First-generation hybrid MEMS gas chromatograph, Lab Chip 5 (2005) 1123–1131.
[6] M. Zhou, J. Lee, H. Zhu, R. Nidetz, K. Kurabayashi, X. Fan, A fully automated portable gas chromatography system for sensitive and rapid quantification of volatile organic compounds in water, RSC Adv. 6 (2016) 49416–49424.
[7] D. Gaddes, J. Westland, F.L. Dorman, S. Tadigadapa, Improved micromachined column design and fluidic interconnects for programmed high-temperature gas chromatography separations, J. Chromatogr. A 1349 (2014) 96–104.
[8] M. Akbar, M. Restaino, M. Agah, Chip-scale gas chromatography: from injection through detection, Microsyst. Nanoeng. 1 (2015) 15039.
[9] C.M. Matzke, R.J. Kottenstette, S.A. Casalnuovo, G.C. Frye-Mason, M.L. Hudson, D.Y. Sasaki, R.P. Manginell, C.C. Wong, Microfabricated silicon gas chromatographic microchannels: fabrication and performance, in: Proc. SPIE 3511, Micromachining and Microfabrication Process Technology IV, 31 August 1998, 1998, http://dx.doi.org/10.1117/12.324309.
[10] B.C. Kaanta, H. Chen, X. Zhang, A monolithically fabricated gas chromatography separation column with an integrated high sensitivity thermal conductivity detector, J. Micromech. Microeng. 20 (2010) 055016.
[11] A.D. Radadia, R.D. Morgan, R.I. Masel, M.A. Shannon, Partially buried microcolumns for micro gas analyzers, Anal. Chem. 81 (2009) 3471–3477.
[12] S. Ali, M. Ashraf-Khorassani, L.T. Taylor, M. Agah, MEMS-based semi-packed gas chromatography columns, Sens. Actuators B 141 (2009) 309–315.
[13] A.C. Lewis, J.F. Hamilton, C.N. Rhodes, J. Halliday, K.D. Bartle, P. Homewood, R.J. Grenfell, B. Goody, A.M. Harling, P. Brewer, Microfabricated planar glass gas chromatography with photoionization detection, J. Chromatogr. A 1217 (2010) 768–774.
[14] S. Jespers, S. Schlautmann, H. Gardeniers, W. De Malsche, F. Lynen, G. Desmet, Chip-based multicapillary column with maximal interconnectivity to combine maximum efficiency and maximum loadability, Anal. Chem. 89 (2017) 11605–11613.
[15] T. Nakai, S. Nishiyama, M. Shuzo, J. Delaunay, I. Yamada, Micro-fabricated semi-packed column for gas chromatography by using functionalized parylene as a stationary phase, J. Micromech. Microeng. 19 (2009) 065032.
[16] A. Wang, S. Hynynen, A.R. Hawkins, S.E. Tolley, H.D. Tolley, M.L. Lee, Axial thermal gradients in microchip gas chromatography, J. Chromatogr. A 1374 (2014) 216–223.
[17] M. Stadermann, A.D. McBrady, B. Dick, V.R. Reid, A. Noy, R.E. Synovec, O. Bakajin, Ultrafast gas chromatography on single-wall carbon nanotube stationary phases in microfabricated channels, Anal. Chem. 78 (2006) 5639–5644.
[18] R. Haudebourg, J. Vial, D. Thiebaut, K. Danaie, J. Breviere, P. Sassiat, I. Azzouz, B. Bourlon, Temperature-programmed sputtered micromachined gas chromatography columns: an approach to fast separations in oilfield applications, Anal. Chem. 85 (2012) 114–120.
[19] D. Wang, H. Shakeel, J. Lovette, G.W. Rice, J.R. Heflin, M. Agah, Highly stable surface functionalization of microgas chromatography columns using layer-by-layer self-assembly of silica nanoparticles, Anal. Chem. 85 (2013) 8135–8141.
[20] H. Shakeel, G.W. Rice, M. Agah, Semipacked columns with atomic layer-deposited alumina as a stationary phase, Sens. Actuators B 203 (2014) 641–646.
[21] R. Haudebourg, Z. Matouk, E. Zoghlami, I. Azzouz, K. Danaie, P. Sassiat, D. Thiebaut, J. Vial, Sputtered alumina as a novel stationary phase for micro machined gas chromatography columns, Anal. Bioanal. Chem. 406 (2014) 1245–1247.
[22] H. Shakeel, D. Wang, J.R. Heflin, M. Agah, Improved self-assembled thiol stationary phases in microfluidic gas separation columns, Sens. Actuators B 216 (2015) 349–357.
[23] M.A. Zareian-Jahromi, M. Ashraf-Khorassani, L.T. Taylor, M. Agah, Design, modeling, and fabrication of MEMS-based multicapillary gas chromatographic columns, J. Microelectromech. Syst. 18 (2009) 28–37.
[24] V.R. Reid, M. Stadermann, O. Bakajin, R.E. Synovec, High-speed, temperature programmable gas chromatography utilizing a microfabricated chip with an improved carbon nanotube stationary phase, Talanta 77 (2009) 1420–1425.
[25] R.R. Reston, E. Kolesar, Silicon-micromachined gas chromatography system used to separate and detect ammonia and nitrogen dioxide. I. Design, fabrication, and integration of the gas chromatography system, J. Microelectromech. Syst. 3 (1994) 134–146.
[26] G. Frye-Mason, R. Kottenstette, P. Lewis, E. Heller, R. Manginell, D. Adkins, G. Dulleck, D. Martinez, D. Sasaki, C. Mowry, Hand-held miniature chemical analysis system (μChemLab) for detection of trace concentrations of gas phase analytes, in: Micro Total Analysis Systems 2000, Springer, 2000, pp. 229–232.
[27] J.J. Whiting, C.S. Fix, J.M. Anderson, A.W. Staton, R.P. Manginell, D.R. Wheeler, E.B. Myers, M.L. Roukes, R. Simonson, High-speed two-dimensional gas chromatography using microfabricated GC columns combined with nanoelectromechanical mass sensors, Solid-State Sensors, Actuators and Microsystems Conference, 2009. TRANSDUCERS 2009. International, IEEE (2009), pp. 1666-1669.
[28] W.R. Collin, A. Bondy, D. Paul, K. Kurabayashi, E.T. Zellers, μGC× μGC: comprehensive two-dimensional gas chromatographic separations with microfabricated components, Anal. Chem. 87 (2015) 1630–1637.
[29] M. Navaei, A. Mahdavifar, J. Xu, J. Dimandja, G. McMurray, P. Hesketh, Micro-fabrication of all silicon 3 meter GC columns using gold eutectic fusion bonding, ECS J. Solid State Sci. Technol. 4 (2015) S3011–S3015.
[30] A. Ghosh, J.E. Johnson, J.G. Nuss, B.A. Stark, A.R. Hawkins, L.T. Tolley, B.D. Iverson, H.D. Tolley, M.L. Lee, Extending the upper temperature range of gas chromatography with all-silicon microchip columns using a heater/clamp assembly, J. Chromatogr. A 1517 (2017) 134–141.
[31] Z. Lin, N. Nuñovero, J. Wang, R. Nidetz, S. Buggaveeti, K. Kurabayashi, E.T. Zellers, A zone-heated gas chromatographic microcolumn: energy efficiency, Sens. Actuators B 254 (2018) 561–572.
[32] A. Bhushan, D. Yemane, D. Trudell, E.B. Overton, J. Goettert, Fabrication of micro-gas chromatograph columns for fast chromatography, Microsyst. Technol. 13 (2007) 361–368.
[33] H.-S. Noh, P.J. Hesketh, G.C. Frye-Mason, Parylene gas chromatographic column for rapid thermal cycling, J. Microelectromech. Syst. 11 (2002) 718–725.
[34] J. Lee, M. Zhou, H. Zhu, R. Nidetz, K. Kurabayashi, X. Fan, Fully automated portable comprehensive 2-dimensional gas chromatography device, Anal. Chem. 88 (2016) 10266–10274.
[35] W.R. Collin, G. Serrano, L.K. Wright, H. Chang, Ns. Nun˜overo, E.T. Zellers, Microfabricated gas chromatograph for rapid, trace-level determinations of gas-phase explosive marker compounds, Anal. Chem. 86 (2013) 655–663.
[36] M. Kim, S. Mitra, A microfabricated microconcentrator for sensors andgas chromatography, J. Chromatogr. A 996 (2003) 1–11.
[37] W.-C. Tian, S.W. Pang, C.-J. Lu, E.T. Zellers, Microfabricated preconcentrator-focuser for a microscale gas chromatograph, J. Microelectromech. Syst. 12 (2003) 264–272.
[38] B. Alfeeli, D. Cho, M. Ashraf-Khorassani, L.T. Taylor, M. Agah, MEMS-based multi-inlet/outlet preconcentrator coated by inkjet printing of polymer adsorbents, Sens. Actuators B 133 (2008) 24–32.
[39] C.Y. Lee, R. Sharma, A.D. Radadia, R.I. Masel, M.S. Strano, On-chip micro gas chromatograph enabled by a noncovalently functionalized single-walled carbon nanotube sensor array, Angew. Chem. Int. Ed. 47 (2008) 5018–5021.
[40] S. Narayanan, G. Rice, M. Agah, Characterization of a micro-helium discharge detector for gas chromatography, Sens. Actuators B 206 (2015) 190–197.
[41] Q.-Y. Cai, E.T. Zellers, Dual-chemiresistor GC detector employing monolayer-protected metal nanocluster interfaces, Anal. Chem. 74 (2002) 3533–3539.
[42] S.I. Shopova, I.M. White, Y. Sun, H. Zhu, X. Fan, G. Frye-Mason, A. Thompson, S.-j. Ja, On-column micro gas chromatography detection with capillary-based optical ring resonators, Anal. Chem. 80 (2008) 2232–2238.
[43] K. Reddy, Y. Guo, J. Liu, W. Lee, M.K.K. Oo, X. Fan, Rapid, sensitive, and multiplexed on-chip optical sensors for micro-gas chromatography, Lab Chip 12 (2012) 901–905.
[44] Y. Qin, Y.B. Gianchandani, A fully electronic microfabricated gas chromatograph with complementary capacitive detectors for indoor pollutants, Microsyst. Nanoeng. 2 (2016) 15049.
[45] Defiant Technologies, FROG-500, http://www.defiant-tech.com/frog-5000-portable-gas-chromatograph.php. (Accessed 20 March 2018).
[46] INFICON, http://products.inficon.com/en-us/product/detail/micro-gc-fusion-gas-analyzer/. (Accessed 20 March 2018).
[47] Electronic Sensor Technology, http://www.estcal.com/buy/portable-znoser. (Accessed 20 March 2018).
[48] APIX Analytics, http://www.apixanalytics.com/chrompix/. (Accessed 20 March 2018).
[49] NANOVA Environmental, https://www.nanovaenv.com/technology/. (Accessed 20 March 2018).
[50] G.E. Spangler, Height equivalent to a theoretical plate theory for rectangular GC columns, Anal. Chem. 70 (1998) 4805–4816.
[51] L.W. Hantao, A. Najafi, C. Zhang, F. Augusto, J.L. Anderson, Tuning the selectivity of ionic liquid stationary phases for enhanced separation of nonpolar analytes in kerosene using multidimensional gas chromatography, Anal. Chem. 86 (2014) 3717–3721.
[52] J.L. Anderson, D.W. Armstrong, Immobilized ionic liquids as high-selectivity/high-temperature/high-stability gas chromatography stationary phases, Anal. Chem. 77 (2005) 6453–6462.
[53] J.L. Anderson, J. Ding, T. Welton, D.W. Armstrong, Characterizing ionic liquids on the basis of multiple solvation interactions, J. Am. Chem. Soc. 124 (2002) 14247–14254.
[54] X. Han, D.W. Armstrong, Ionic liquids in separations, Acc. Chem. Res. 40 (2007) 1079–1086.
[55] J. Ding, T. Welton, D.W. Armstrong, Chiral ionic liquids as stationary phases in gas chromatography, Anal. Chem. 76 (2004) 6819–6822.
[56] K. Dettmer, Assessment of ionic liquid stationary phases for the GC analysis of fatty acid methyl esters, Anal. Bioanal. Chem. 406 (2014) 4931–4939.
[57] C. Ragonese, D. Sciarrone, P.Q. Tranchida, P. Dugo, G. Dugo, L. Mondello, Evaluation of a medium-polarity ionic liquid stationary phase in the analysis of flavor and fragrance compounds, Anal. Chem. 83 (2011) 7947–7954.
[58] B.M. Weber, P. Walsh, J.J. Harynuk, Determination of hydrocarbon group-type of diesel fuels by gas chromatography with vacuum ultraviolet detection, Anal. Chem. 88 (2016) 5809–5817.
[59] C.F. Poole, N. Lenca, Gas chromatography on wall-coated open-tubular columns with ionic liquid stationary phases, J. Chromatogr. A 1357 (2014) 87–109.
[60] B.P. Regmi, R. Chan, M. Agah, Ionic liquid functionalization of semi-packed columns for high-performance gas chromatographic separations, J. Chromatogr. A 1510 (2017) 66–72.
[61] G. Serrano, S.M. Reidy, E.T. Zellers, Assessing the reliability of wall-coated microfabricated gas chromatographic separation columns, Sens. Actuators B 141 (2009) 217–226.

[62] S. Reidy, G. Lambertus, J. Reece, R. Sacks, High-performance, static-coated silicon microfabricated columns for gas chromatography, Anal. Chem. 78 (2006) 2623–2630.
[63] S. Aldrich, Supleco Ionic Liquid GC Columns Applications, 2014.
[64] J.V. Hinshaw, Pinning down tailing peaks, LC GC Eur. 22 (2009) 310–314.
[65] Y. Li, X. Du, Y. Wang, H. Tai, D. Qiu, Q. Lin, Y. Jiang, Improvement of column efficiency in MEMS-based gas chromatography column, RSC Adv. 4 (2014) 3742–3747.
[66] J.W. Dolan, Peak tailing and resolution, LCGC North Am. 20 (2002) 430–437.
[67] M.H. Abraham, Scales of solute hydrogen-bonding: their construction and application to physicochemical and biochemical processes, Chem. Soc. Rev. 22 (1993) 73–83.
[68] P. Twu, Q. Zhao, W.R. Pitner, W.E. Acree, G.A. Baker, J.L. Anderson, Evaluating the solvation properties of functionalized ionic liquids with varied cation/anion composition using the solvation parameter model, J. Chromatogr. A 1218 (2011) 5311–5318.
[69] J. Krupčík, R. Gorovenko, I. Špánik, I. Bočková, P. Sandra, D.W. Armstrong, On the use of ionic liquid capillary columns for analysis of aromatic hydrocarbons in low-boiling petrochemical products by one-dimensional and comprehensive two-dimensional gas chromatography, J. Chromatogr. A 1301 (2013) 225–236.
[70] L. Ugena, S. Moncayo, S. Manzoor, D. Rosales, J. Cáceres, Identification and discrimination of brands of fuels by gas chromatography and neural networks algorithm in forensic research, J. Anal. Methods Chem. 2016 (2016).
[71] L.A.F. de Godoy, E.C. Ferreira, M.P. Pedroso, C.Hd.V. Fidélis, F. Augusto, R.J. Poppi, Quantification of kerosene in gasoline by comprehensive two-dimensional gas chromatography and N-way multivariate analysis, Anal. Lett. 41 (2008) 1603–1614.
[72] C. Ragonese, P.Q. Tranchida, D. Sciarrone, L. Mondello, Conventional and fast gas chromatography analysis of biodiesel blends using an ionic liquid stationary phase, J. Chromatogr. A 1216 (2009) 8992–8997.
[73] R.O. Keto, P.L. Wineman, Detection of petroleum-based accelerants in fire debris by target compound gas chromatography/mass spectrometry, Anal. Chem. 63 (1991) 1964–1971.
[74] J.E. Nichols, M.E. Harries, T.M. Lovestead, T.J. Bruno, Analysis of arson fire debris by low temperature dynamic headspace adsorption porous layer open tubular columns, J. Chromatogr. A 1334 (2014) 126–138.
[75] E. Stauffer, D. Byron, Alternative fuels in fire debris analysis: biodiesel basics, J. Forensic Sci. 52 (2007) 371–379.
[76] J.D. McCurry, GC analysis of total fatty acid methyl esters (FAME) and methyl linolenate in biodiesel using the revised EN14103:2011 method, Agilent Technol. (2012). https://www.agilent.com/cs/library/applications/5991-0441EN.pdf.